PAPER

Hexamethylenetetramine-based ionic liquid/MIL-101(Cr) metal–organic framework composite: a novel and versatile tool for the preparation of pyrido[2,3-*d*:5,6-*d′*]dipyrimidines†

Boshra Mirhosseini-Eshkevari,[ab] Mohammad Ali Ghasemzadeh, [ID] *[b]
Manzarbanoo Esnaashari*[a] and Saeed Taghvaei Ganjali[a]

In the current paper, a hexamethylenetetramine-based ionic liquid immobilized on the MIL-101(Cr) metal–organic framework was successfully synthesized as a novel, efficient, and recoverable catalyst for the synthesis of pyrido[2,3-*d*:5,6-*d′*]dipyrimidine derivatives *via* the reaction of barbituric acid derivatives, 6-aminouracil/6-amino-1,3-dimethyl uracil, and aromatic aldehydes under solvent-free conditions. Characterization of the catalyst was carried out using various methods such as field emission scanning electron microscopy (FE-SEM), energy-dispersive X-ray spectroscopy (EDS), X-ray diffraction (XRD), thermogravimetric analysis (TGA), Fourier transform infrared spectrophotometry (FT-IR), and Brunauer–Emmett–Teller (BET). Efficient transformation, short reaction times, excellent yields, easy product isolation, mild conditions, and the potential high recyclability of the organocatalyst are the main features of this protocol.

1. Introduction

Currently, inorganic clusters or metal ions (usually transition metal) are used to make solid compounds that are crystalline in structure, connecting to two or multifunctional organic elements for providing metal–organic frameworks (MOFs).[1] Metal–organic frameworks have, in past years, been useful resources for their applications in preparing different catalysts, fuel cells, electronics, sensors, and extensive industrial products, together with their other use in drug delivery, selective separation, adsorption, and petrochemistry.[2–4] High surface area and thermal stability are some benefits of these porous and nanoscopic materials.[5–8] MIL-101 is one of the most promising porous materials for future energy and environmental applications, owing to its superior physicochemical properties including high hydrothermal/chemical stability and desirable textural properties.[9] MIL-101 is a member of the large family of MOFs with the largest Langmuir surface area (4500 m^2 g^{-1}), pore size (29–34 Å), and cell volume (702.000 Å).[10] Several probabilities to model the porous complexity of MOFs in a logical method have been offered by multivariate MOFs (MTV-
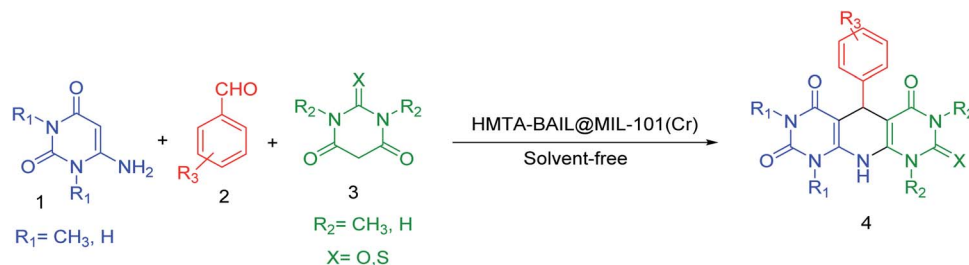
MOFs), merging several nuclei, organic, and linker characteristics into a framework.[11–13] Some other cases regarding carbon–carbon bond formation, oxidation reactions, and catalytic activity of MOFs have also been reported.[14,15] The reusable rigid acid catalysts have recently been substantially replaced in industrial operations by dangerous homogeneous acid catalysts.[16,17] By filtering or centrifuging, acidic heterogeneous catalyzing agents may be isolated efficiently from the reaction blend without a need for particular treatments, thus providing a promising ecological process and reducing the handling cost.[18] The reusability is another advantage of the heterogeneous catalyst.[19,20] Ionic liquids (ILs), consisting of ions, may have certain features; therefore, they are used broadly in different organic synthesis and catalytic reactions. ILs have further been allocated as a group of environmental materials owing to their non-flammable features, besides low vapor pressure.[21] Cases of their uses as catalysts in Biginelli reaction have also recently been discussed, showing excellent catalytic activity.[22,23] Although ample prospects are in using MOFs as solid supports of ILs, ILs/MOFs composites have revealed significant features due to the ILs nano sizing than the bulk ionic liquid, indicating the typical freezing or melting features.[24] Therefore, preparing and exploring the use of chemically confinement ILs-MOFs for catalysis for the first time is very substantial. One of the most efficient strategies of synthesization of organic and medicinal chemistry products is multicomponent reactions (MCRs).[25] A substantial group of annulated uracils is derivatives of pyridopyrimidine that, with a wide variety of medicinal, pharmacological, and biological features, have recently

[a]Department of Chemistry, North Tehran Branch, Islamic Azad University, Post Box: 1913674711, Tehran, I. R. Iran. E-mail: Mb_esnaashari@yahoo.com
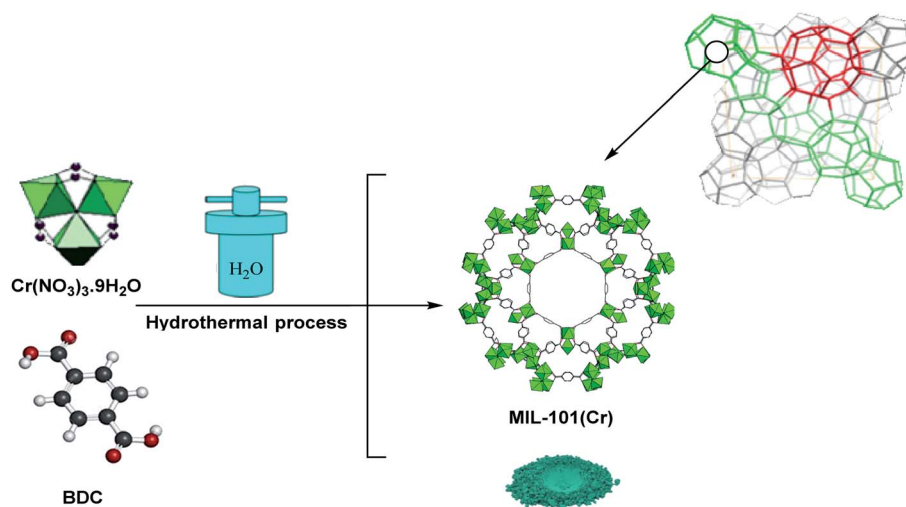
[b]Department of Chemistry, Qom Branch, Islamic Azad University, Post Box: 37491-13191, Qom, I. R. Iran. E-mail: Ghasemzadeh@qom-iau.ac.ir; Fax: +98-253-7780001; Tel: +98-253-7780001

Scheme 1 Synthesis of pyrido[2,3-d:5,6-d′]dipyrimidine derivatives using HMTA-BAIL@MIL-101(Cr) under solvent-free conditions.

Scheme 2 Preparation of MIL-101(Cr).

gained significant attention.[26,27] Pyrido [2,3-d:6,5-d′]dipyrimidines is synthesized by various catalysts like piperidine,[28] SBA-Pr-SO$_3$H,[29] P$_2$O$_5$ (ref. 30) and MWCNTs@L-His/Cu(II).[31]

These protocols have some advantages including high product yields, short reaction times, and mild reaction conditions while they have some drawbacks such as high production costs, low chemical and thermal stability, and tedious work-up. Therefore, there is a considerable attempt to build an appropriate catalytic system to synthesize pyrido[2,3-d:5,6-d′]dipyrimidine. Recently, we have reported various synthetic methods for the preparation of several heterocycle compounds using nanocatalysts.[32–36] In experimental and industrial research, it is essential to decrease toxic waste and reaction process time to protect the environment.
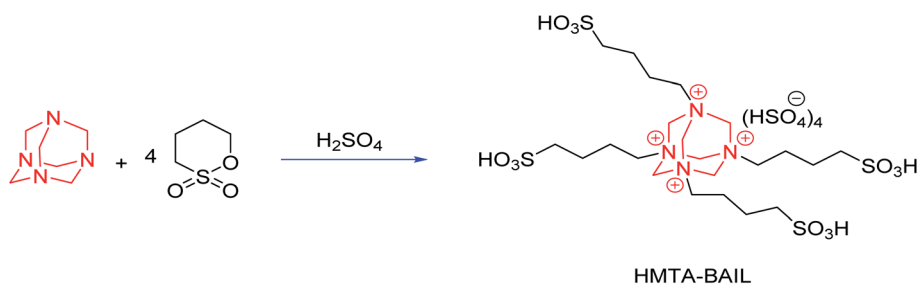
In this research, we decided to investigate the application of HMTA-BAIL@MIL-101(Cr) as a novel Brønsted acidic ionic

liquid, highly efficient and reusable catalyst for the synthesis of pyrido[2,3-d:5,6-d′]dipyrimidine derivatives *via* the one-pot three-component condensation reaction of 6-aminouracil or 6-amino-1,3-dimethyl uracil, barbituric acid derivatives and aromatic aldehydes under solvent-free conditions (Scheme 1).
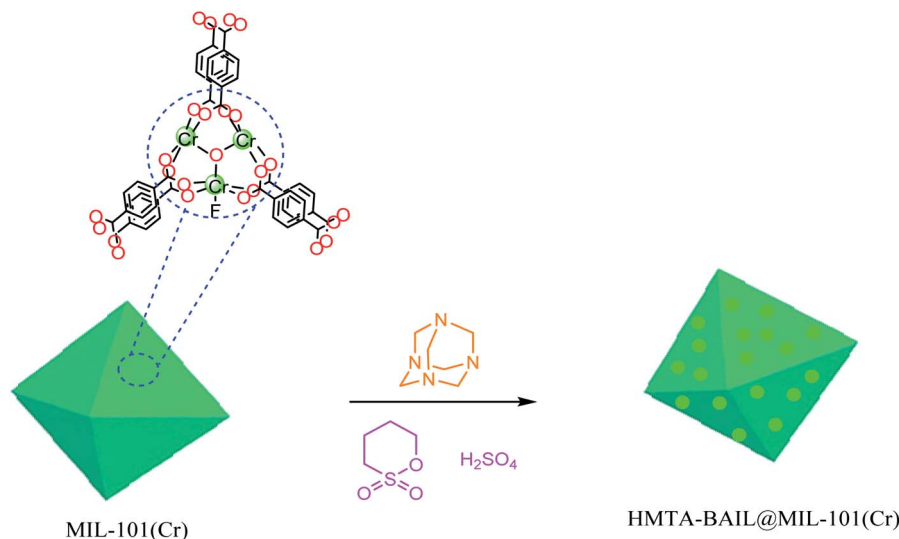
2. Experimental

2.1 Materials and instrumentation

The high purities chemicals were bought from Sigma-Aldrich and Merck. The substances with the commercial reagent grades were utilized with no more purifying. The melting point was unmodified and defined in a capillary tube over a melting point microscope (Boetius). ^{1}H NMR and ^{13}C NMR spectra were attained on Bruker 250 MHz spectrometer with DMSO-d_6 as a solvent and utilizing TMS as

Scheme 3 Preparation of HMTA-BAIL.

Scheme 4   Preparation of HMTA-BAIL@MIL-101(Cr).

an internal standard. Recording FT-IR spectra was performed on Magna-IR, spectrometer 550. The elemental analyses (H, C, N) were conducted using a Carlo ERBA Model EA 1108 analyzer. Powder XRD (X-ray diffraction) was performed on a Philips diffractometer (X'pert Co.) with Cu Kα mono chromatized radiation ($\lambda = 1.5406$ Å). The microscopic morphology of the products was observed through SEM (LEO, 1455VP). Recording the mass spectra was based on a Joel D-30 tool at an ionizing potential of 70 eV. The energy dispersive analysis of X-ray was used to perform compositional analysis (EDX, Kevex, Delta Class 1). A Mettler Toledo TGA was considered to perform thermogravimetric analysis (TGA), under argon and heating was performed to 825 °C from room temperature. A Belsorp mini automatic adsorption tool was used to measure nitrogen adsorption–desorption isotherms at 196 °C followed by degassing the specimens for 5 h at 150 °C. The sample weight was estimated as 10 mg in the TG test with heating at 10 °C per minute.

2.2   Preparation of MIL-101(Cr)

Scheme 2 illustrates the synthesis procedure of the MIL-101(Cr), which was performed under hydrothermal conditions based on

a previously used procedure with minor modification.[37] To this end, a combination of 5.4 g of $Cr(NO_3)_3 \cdot 9H_2O$, 1.5 g of terephthalic acid (BDC), 45 mL of deionized water, and 0.6 mL of hydrofluoric acid (5 mol L^{-1}) was sonicated for 10 min and then the mixture was transferred to a Teflon-lined stainless steel autoclave for 8 h at 220 °C. Subsequent to cooling down the autoclave to ambient temperature, the reaction mixture was subjected to filtration and washing by distilled water. The resultant solid was dehydrated in an 80 °C oven nightlong and denoted as crude MIL-101(Cr) crystals.

2.3   Preparation of HMTA-BAIL

HMTA-BAIL was prepared based on the previous method with a slight modification.[38] A mixture of hexamethylenetetramine (0.01 mol) and 1,4-butane sultone (0.08 mol) was stirred at room temperature for 72 h under solvent-free conditions. The produced white solid zwitterion (HMTA-BAIL precursor) was filtered out and washed repeatedly by diethyl ether. An ionic liquid was formed through adding a stoichiometric quantity of sulfuric acid to the zwitterion and then stirring the produced
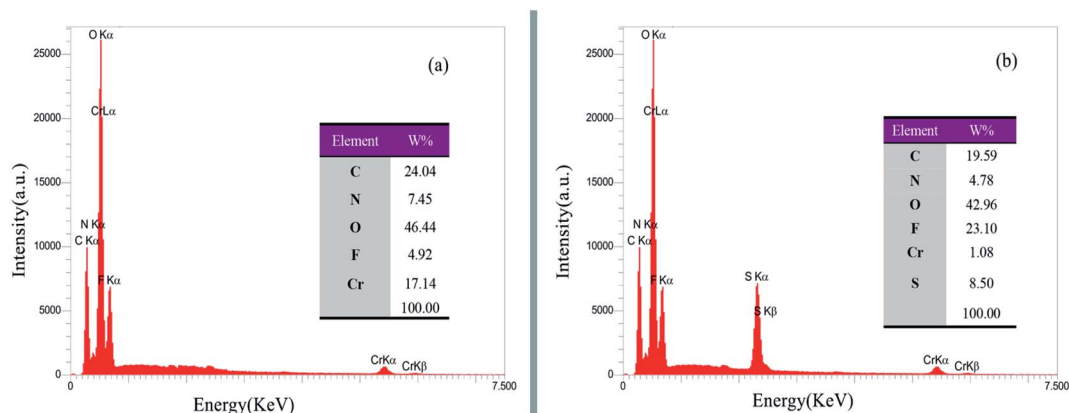

Fig. 1   The EDS spectra of MIL-101(Cr) (a) and HMTA-BAIL@MIL-101(Cr) (b).
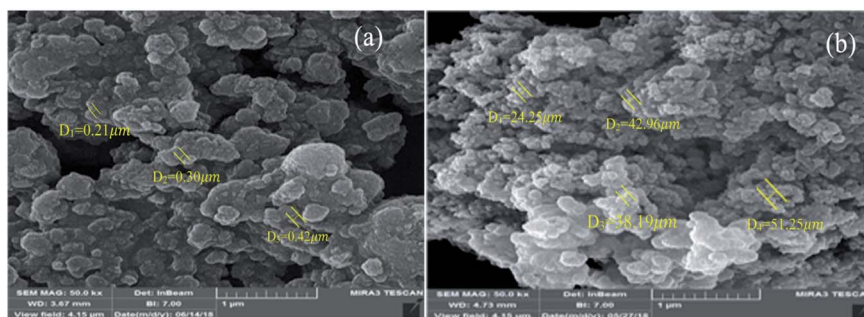
Fig. 2 FE-SEM images of MIL-101(Cr) (a) and HMTA-BAIL@MIL-101(Cr) (b).

admixture at 90 °C for 8 h. Lastly, washing the BAIL phase was performed for different times by diethyl ether and toluene for removing non-ionic remains, and then dehydrating was performed at 100 °C under vacuum (Scheme 3).

2.4 Preparation of HMTA-BAIL@MIL-101(Cr)

Scheme 4 displays the preparing procedure of the new and vigorous Brönsted acidic ionic liquid functionalized MIL-101(Cr) MOF. In brief, dehydration of MIL-101(Cr) (1.0 g) was done under vacuum at 110 °C for 12 h. A suspension of MIL-101(Cr) in anhydrous toluene (30 mL) was prepared in a round bottom flask, and hexamethylenetetramine (5 mmol) was added afterward. The reaction combinations were refluxed through stirring for 12 h at 80 °C. To separate the solvent, it was filtrated upon the termination of the reaction, and then washed by toluene to remove the extra hexamethylenetetramine. Thereafter, the product was dissipated in 30 mL of anhydrous toluene. Throughout stirring vigorously, an equal molar ratio 1,4-butane sultone (5 mmol) was incorporated into the solution, followed by refluxing the admixture for 12 h at 80 °C. Finally, the solid was harvested via filtration and dehydrated under vacuum for 3 h at 110 °C. A suspension of the solid was then made in 20 mL of ethanol simultaneously an equivalent amount of concentrated H_2SO_4 (98%) was added dropwise for 24 h at 50 °C. In the end, the catalyst was isolated by filtration and desiccated under vacuum for 12 h at 50 °C.

2.5 General procedure for the synthesis of pyrido[2,3-d:5,6-d']dipyrimidine(4a–4p)

A combination of 6-aminouracil/6-amino-1,3-dimethyl uracil (1 mmol), barbituric acid derivatives (1 mmol), aldehyde (1 mmol), and HMTA-BAIL@MIL-101(Cr) (0.008 g) was heated at 80 °C for 10–15 min. Followed by completing the reaction based on the TLC (hexane/ethyl acetate, 4 : 1) (thin layer chromatography), cooling the reaction combination was performed to room temperature and the achieved solid was dissolved within dichloromethane. Then, the catalyst was not soluble in CH_2Cl_2 and was separated through simple filtration. Evaporating the solvent was performed and recrystallizing the residue from ethanol was performed to obtain the pure product.

Spectral data of the new products are given below.

5-(5-Bromo-2-hydroxyphenyl)-7,9-dimethyl-8-thioxo-5,8,9,10-tetrahydropyrido[2,3-d:6,5-d']dipyrimidine-2,4,6(1H,3H,7H)-trione (4o). White solid; mp: >300 °C. ^1H NMR (250 MHz, DMSO-d_6)

δ: 3.01 (s, 3H, CH₃), 3.66 (s, 3H, CH₃), 4.22 (s, 1H, CH), 6.96–6.99 (d, 1H, J = 7.4 Hz, ArH), 7.07 (s, 1H, ArH), 7.30–7.33 (d, 1H, J = 7.8 Hz, ArH), 9.27 (s, 1H, OH), 10.40 (s, 1H, NH), 10.64 (s, 1H, NH), 11.58 (s, 1H, NH); ^{13}C NMR (62.9 MHz, DMSO-d_6) δ: 27.49, 31.76, 50.39, 82.52, 97.14, 114.97, 118.79, 123.66, 129.29, 131.61, 135.34, 146.33, 150.33, 151.57, 152.85, 157.33, 162.33. FT-IR (KBr): 3365, 3172, 3051, 1705, 1674, 1591 cm^{-1}; anal. calcd. For $C_{17}H_{14}BrN_5O_4S$: C 50.80, H 3.62, Br 7.50, N 17.77, O 13.53, S 6.78. Found C 50.76, H 3.61, Br 7.53, N 17.74, O 13.46, S 6.64.; MS (EI) (m/z): 462.99 (M⁺).

5-(2-Hydroxy-5-nitrophenyl)-1,3-dimethyl-8-thioxo-5,8,9,10-tetrahydropyrido[2,3-d:6,5-d']dipyrimidine-2,4,6(1H,3H,7H)-trione (4p). White solid; mp: >300 °C. · ^1H NMR (250 MHz, DMSO-d_6) δ: 3.09 (s, 3H, CH₃), 3.22 (s, 3H, CH₃), 4.13 (s, 1H, CH), 6.73 (d, 1H, J = 7.4 Hz, ArH), 7.11 (d, 1H, J = 7.7 Hz, ArH), 7.19 (d, 1H, J = 7.8 Hz, ArH), 9.12 (s, 1H, OH); 9.18 (s, 1H, NH), 10.28 (s, 1H, NH), 11.12 (s, 1H, NH); ^{13}C NMR (62.9 MHz, DMSO-d_6) δ: 27.64, 33.24, 50.53, 82.52, 97.68, 116.51, 121.32, 123.53, 126.94, 128.65, 135.82, 146.86, 150.74, 151.57, 152.43, 157.24, 162.45. FT-IR (KBr): 3456, 3444, 3107, 2951, 1693, 1668, 1597 cm^{-1}; anal. calcd. For $C_{17}H_{14}N_6O_6S$: C 47.44, H 3.28, N 19.53, O 22.30, S 7.45. Found C 47.42, H 3.31, N 19.51, O 22.32, S 7.42.; MS (EI) (m/z): 430.07 (M⁺).

3. Results and discussion

The prepared catalyst was analyzed through some characterization methods such as EDS, FE-SEM, XRD, FT-IR, BET, and TGA.
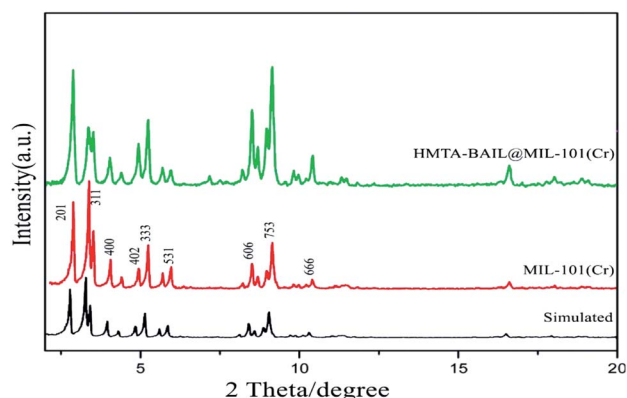

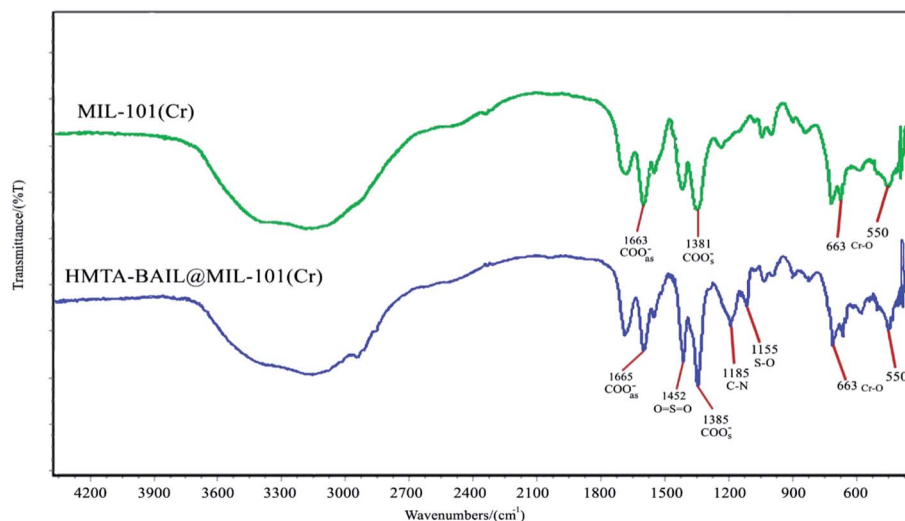**Fig. 3** XRD patterns of MIL-101(Cr) and HMTA-BAIL@MIL-101(Cr).

Fig. 4 The FT-IR spectra of MIL-101(Cr) and HMTA-BAIL@MIL-101(Cr).

3.1 EDS analysis

Fig. 1 illustrates the elemental analysis of the MIL-101(Cr) and HMTA-BAIL@MIL-101(Cr) obtained from EDS. The results confirmed the existence of C, O, Cr, F and N as the only elementary components of MIL-101(Cr) MOF (Fig. 1a). In EDS spectrum of HMTA-BAIL@MIL-101(Cr), C, O, Cr, F, N and S elements were observed (Fig. 1b). The presence of the S element in the Fig. 1b confirmed the successful functionalization of the ionic liquid.

3.2 FE-SEM analysis

To distinguish the particle size and surface morphology of the synthesized HMTA-BAIL@MIL-101(Cr) SEM was studied. Fig. 2a and b show an FE-SEM micrograph of the as-synthesized MIL-101(Cr) and HMTA-BAIL@MIL-101(Cr) representing a characteristic octahedral shape form.

3.3 Powder X-ray diffraction

The PXRD (powder X-ray diffraction) patterns of the BAIL functionalized MIL-101(Cr) substances represent nearly all the main diffraction peaks regarding the pure MIL-101(Cr) and simulated pattern (Fig. 3). Such findings showed that the MIL-101(Cr) materials' crystalline structures were unaffected and remained intact over the BAIL functionalization procedure. The reflection planes equivalent to the Miller indices (201), (311), (440), (402), (333), (531), (606), (753), (666), and (600) are indexed for the MIL-101 consistent with the reported values.[37,39] It is found that there is a good consistency between the representative peaks of the synthesized HMTA-BAIL@MIL-101(Cr) materials and MIL-101(Cr). There is also an agreement between the observations and the one reported in the studies.[40]

3.4 Infrared spectroscopy

The FT-IR spectra of the BAIL-functionalized MIL-101(Cr) and bare MIL-101(Cr) nanostructure are represented in Fig. 4. FT-IR
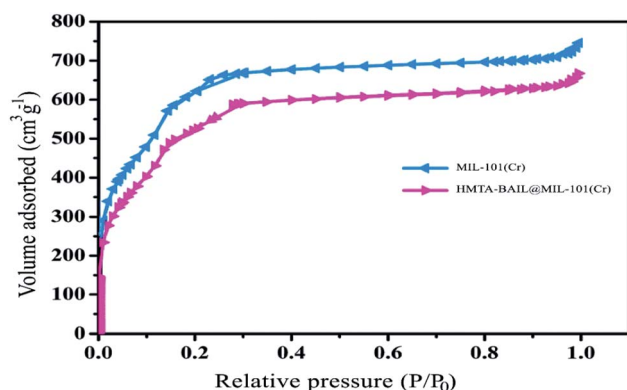

Fig. 5 The N_2 adsorption–desorption isotherms at 77 K of MIL-101(Cr) and HMTA-BAIL@MIL-101(Cr).
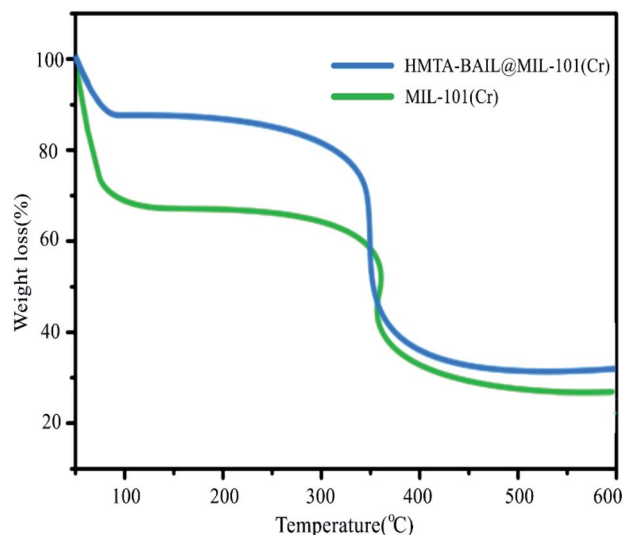

Fig. 6 TGA curves of the MIL-101(Cr) and HMTA-BAIL@MIL-101(Cr) under Ar atmosphere.
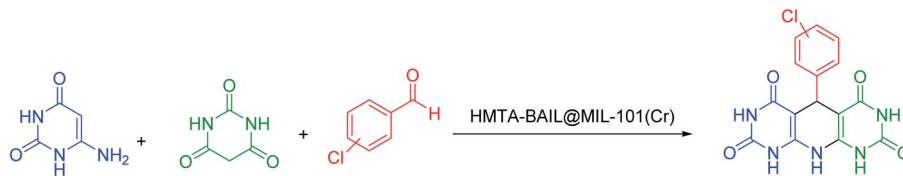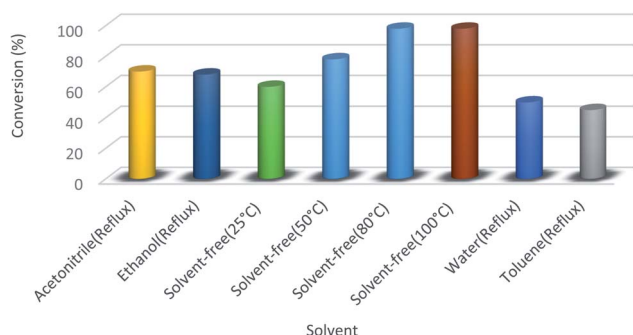
Scheme 5 The model reaction for the synthesis pyrido[2,3-*d*:5,6-*d'*]dipyrimidine **4j**.

Fig. 7 The optimization of the solvent in the model study.

spectrum of MIL-101(Cr) shows the absorption bands at 1381 and 1663 cm^{-1} related to symmetric and asymmetric stretching vibrations of COO–.[41] Moreover, Cr–O bonds are appeared around 550 and 663 cm^{-1}. In addition, the contribution of HMTA-BAIL in the HMTA-BAIL@MIL-101(Cr) composite was verified with the existence of the absorption bands corresponding to hexamethylenetetramine ring and sulfonyl groups. As indicated in FT-IR spectrum of HMTA-BAIL@MIL-101(Cr), the absorption bands at 1155 and 1185 cm^{-1} are corresponding to stretching vibrations of S–O and C–N bonds, respectively. Moreover, the stretching vibrations of O=S=O is appeared at 1452 cm^{-1} confirming that the incorporation of HMTA-BAIL into the MIL-101(Cr).

3.5 BET analysis

The N$_2$ adsorption–desorption isotherm of MIL-101(Cr) and HMTA-BAIL@MIL-101(Cr) was shown in Fig. 5. For the bare MIL-101(Cr) an overall pore volume and BET surface area were

1.42 cm^3 g^{-1} and 2473 m^2 g^{-1}, these values are close to the reported values (pore volume and BET surface area were 1.19 cm^3 g^{-1} and 2338 m^2 g^{-1}, respectively) for MIL-101(Cr).[42] The HMTA-BAIL@MIL-101(Cr) exhibited corresponding values (pore volume and BET surface area) of 1.06 cm^3 g^{-1} and 1921 m^2 g^{-1}. The reduced porosity for HMTA-BAIL@MIL-101(Cr) in comparison with MIL-101(Cr) may be related to the pore blockage of MIL-101(Cr) *via* the BAIL groups.

3.6 TGA analysis

The thermogravimetric analysis curves for MIL-101(Cr) and HMTA-BAIL@MIL-101(Cr) show two-step weight losses at 30 to 100 °C and >300 °C to 400 °C, respectively (Fig. 6). The first loss can be related to the solvent loss in the framework. The subsequent loss can be attributed to decomposing the immobilized ionic liquid moieties into the MIL-101(Cr) nanocages, causing the collapse of frameworks.

In the next step of our research, we decided to evaluate the catalytic activity of the prepared novel catalyst for synthesizing pyrido[2,3-*d*:5,6-*d'*]dipyrimidines. For achieving this purpose, the reaction conditions (solvent, catalyst, and amount of catalyst) were first optimized, while selecting the reaction between 6-aminouracil, barbituric acid, and 4-chlorobenzaldehyde as a model reaction (Scheme 5).

To discover the effects of solvent in preparing pyrido[2,3-*d*:5,6-*d'*]dipyrimidine **4j**, we conducted the model reaction using HMTA-BAIL@MIL-101(Cr) by different solvents as well as solvent-free conditions at various temperatures. As illustrated in Fig. 7, it concluded that solvent-free conditions with high temperatures have great effects on the reaction accelerating. The best findings (98% yield within 10 min) were attained without using any toxic solvent at 80 °C for this multicomponent reaction.
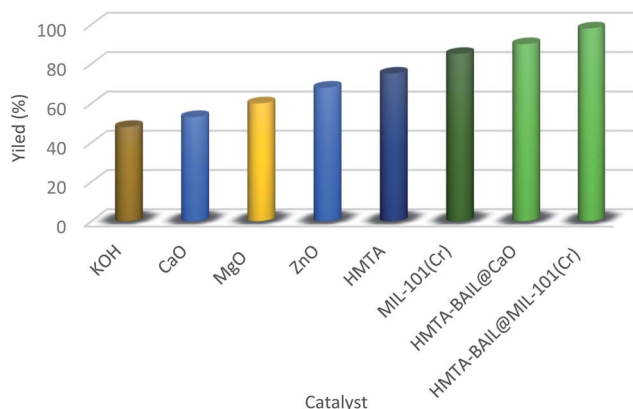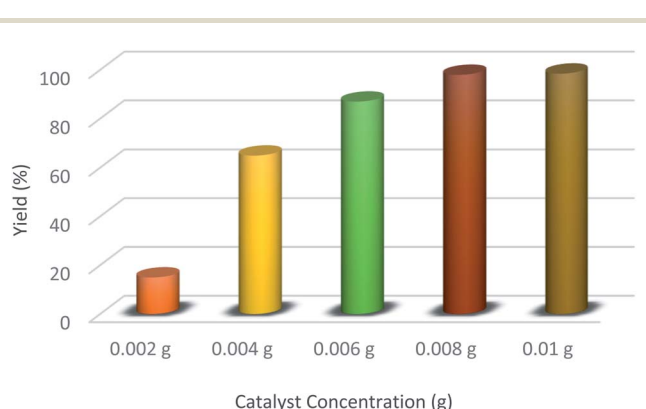
Fig. 8 The effect of various catalysts on model reaction.

Fig. 9 The effect of catalyst amount on the model reaction.

Table 1 Synthesis of pyrido[2,3-d:5,6-d']dipyrimidines using HMTA–BAIL@MIL-101(Cr) catalyst

Entry	R_1	R_2	R_3	X	Product	Time(min)	Yield[a] (%)	Mp °C	Lit. Mp °C
1	CH₃	H	H	O	**4a**	20	91	>300 °C	>300 °C[28]
2	CH₃	H	4-Cl	O	**4b**	14	95	>300 °C	>300 °C[28]
3	CH₃	H	4-NO₂	O	**4c**	15	97	>300 °C	>300 °C[28]
4	CH₃	H	4-CH₃	O	**4d**	16	88	>300 °C	>300 °C[28]
5	H	CH₃	H	O	**4e**	12	92	>300 °C	>300 °C[28]
6	H	CH₃	4-Cl	O	**4f**	20	87	>300 °C	>300 °C[28]
7	H	CH₃	4-NO₂	O	**4g**	10	90	>300 °C	>300 °C[28]
8	H	CH₃	4-CH₃	O	**4h**	18	89	>300 °C	>300 °C[28]
9	H	H	H	O	**4i**	17	93	>300 °C	>300 °C[28]
10	H	H	4-Cl	O	**4j**	10	98	>300 °C	>300 °C[28]
11	H	H	H	S	**4k**	14	93	>300 °C	>300 °C[28]
12	H	H	4-Cl	S	**4l**	16	96	>300 °C	>300 °C[28]
13	H	CH₃	H	S	**4m**	13	91	>300 °C	>300 °C[28]
14	H	H	4-Cl	S	**4n**	15	93	>300 °C	>300 °C[28]
15	H	CH₃	5-Br, 2-OH	S	**4o**	17	95	>300 °C	—[b]
16	CH₃	H	2-OH, 5-NO₂	S	**4p**	19	89	>300 °C	—[b]

[a] Isolated yield. [b] New products.

Table 2 Comparison on the efficiency of HMTA–BAIL@MIL-101(Cr) for the synthesis of pyrido[2,3-d:5,6-d']dipyrimidines[a]

Entry	Catalyst	Conditions	Time/yield (%)	References
1	Piperidine	H₂O/60 °C/U. S.	1 h/81–91	28
2	SBA-Pr-SO₃H	Solvent-free/140 °C	1.5 h/65–90	29
3	P₂O₅	EtOH/reflux	2 h/80–88	30
4	MWCNTs@L-His/Cu(ɪɪ)	EtOH/reflux	1 h/78–92	31
5	HMTA-BAIL@MIL-101(Cr)	Solvent-free, 80 °C	10 min/87–98	This work

[a] Based on the three-component reaction of 6-aminouracil, barbituric acid, 4-chlorobenzaldehyde.

A temperature increase in this reaction represented no significant impacts on time and product yield.

Furthermore, to assess the effects of diverse catalysts, the catalytic performance of seven types of catalysts like KOH, CaO, MgO, ZnO, HMTA, MIL-101(Cr), HMTA-BAIL@CaO and HMTA-BAIL@MIL-101(Cr) was examined on the model reaction under solvent-free conditions (Fig. 8). The results of this study exhibited that HMTA-BAIL@MIL-101(Cr) was afforded pyrido [2,3-d:5,6-d']dipyrimidine **4j** in superior yield within short reaction time compared to the other catalysts.

To continue our study, we ran the reaction of 6-aminouracil, barbituric acid, and 4-chlorobenzaldehyde using different amounts of HMTA-BAIL@MIL-101(Cr) nanocatalyst under solvent-free conditions. According to Fig. 9, the optimum concentration of HMTA-BAIL@MIL-101(Cr) was attained at 0.008 g. The time and yield of the reaction are not altered by a value of higher than 0.008 g.

After examining different conditions on the reaction progress, we found the general applicability of the HMTA-BAIL@MIL-101(Cr) catalyst with aryl aldehydes comprising electron withdrawing or donating substituents, barbituric acid/thiobarbituric acid/1,3-dimethylbarbituric acid and 6-aminouracil or 6-amino-1,3-dimethyl uracil. According to Table 1, all of the derivatives with electron withdrawing or donating groups were afforded the products in good to the superior yields. The total HMTA-

BAIL@MIL-101(Cr) was made to be a highly efficient nano-structure for the synthesis of pyrido[2,3-d:5,6-d']dipyrimidines.

The catalytic performance and efficiency of HMTA-BAIL@MIL-101(Cr) were compared with several previous approaches to synthesize the pyrido[2,3-d:5,6-d']dipyrimidines, presented in Table 2. As indicated, HMTA-BAIL@MIL-101(Cr) nanocomposite is greater based on the reported catalysts regarding reaction time, yield, and conditions. Our method has the advantages of short reaction time, mild conditions, and good to superior yields (Table 2).

3.7 Recycling and reusing of the catalyst

The recovery and recyclability of the HMTA-BAIL@MIL-101(Cr) were also controlled by taking the condensation reaction for the
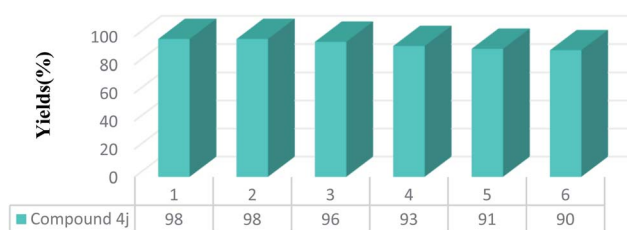

Fig. 10 Reusability of the HMTA–BAIL@MIL-101(Cr) catalyst.

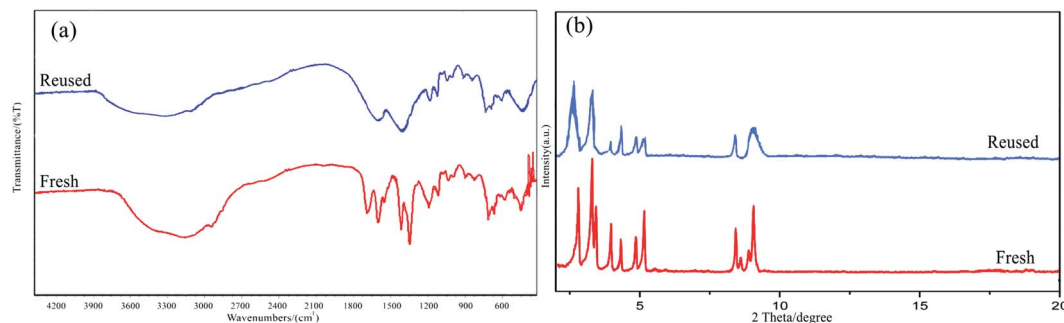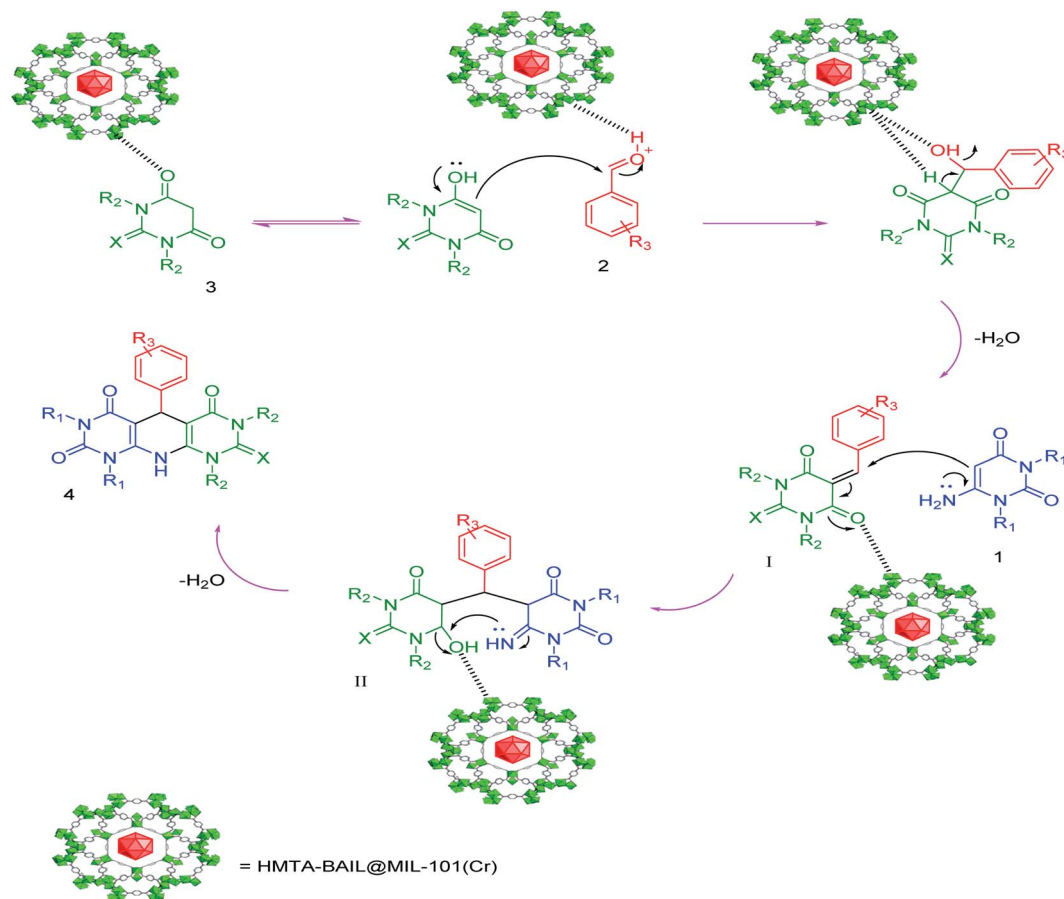|	1	2	3	4	5	6
Compound 4j	98	98	96	93	91	90

Fig. 11 FT-IR spectrum (a) and XRD pattern (b) of the recovered HMTA-BAIL@MIL-101(Cr) after 6 runs.

model reaction. Followed by completing the reaction (based on TLC), dissolving the residues was performed in CH_2Cl_2, while filtering the catalyst. According to Fig. 10, this catalyst could be reused over six runs with no considerable loss of its catalytic activity.

The chemical structure of recovered HMTA-BAIL@MIL-101(Cr) was verified using XRD pattern and FT-IR spectrum. There is no significant difference between the XRD and FT-IR of the fresh and recovered nanocomposite (Fig. 11(a and b)). Also, the acid sites (1.23 mmol g^{-1}) of the catalyst after 6 times reused had no dramatic changes based on the acid–base titration measurement, in comparison with acid sites of the fresh HMTA-

BAIL@MIL-101(Cr) nanocomposite (1.26 mmol g^{-1}). These facts prove that the efficiency, appearance and structure of HMTA-BAIL@MIL-101(Cr) catalyst remained intact in recycles and there was no considerable deformation or leaching after 6 runs.

A plausible mechanism for the synthesis of pyrido[2,3-*d*:5,6-*d'*]dipyrimidines utilizing HMTA-BAIL@MIL-101(Cr) as the catalyst is represented in Scheme 6. The findings were experimentally studied based on the literature.[29,30] It is likely that HMTA-BAIL@MIL-101(Cr) acts as a Brønsted acid and increments the carbonyl group's electrophilicity on the aldehyde by release proton. Firstly, barbituric acid **3** has a reaction with

Scheme 6 Proposed mechanism for the synthesis of pyrido[2,3-*d*:5,6-*d'*]dipyrimidines.

aromatic aldehydes **2** to create standard Knoevenagel condensation product **I**. The succeeding Michael-type adding of the 6-aminouracil **1** with Knoevenagel product **I** after cyclization provides the intermediate **II** giving desired product **4** on dehydration.

4. Conclusions

In conclusion, we have reported a new Brönsted acidic ionic liquid immobilized on MIL-101(Cr) MOF as an efficient nanoporous and heterogeneous catalyst for the synthesis of pyrido [2,3-*d*:5,6-*d'*]dipyrimidine derivatives under solvent-free conditions. The new catalyst was characterized by EDS, SEM, XRD, FT-IR, BET and TGA. The main benefits of this work are the short reaction time, facile workup, reusability of the catalyst, and high yield of products. The highly reactive and heterogeneity nature of this catalyst offers a wide application in heterocyclic synthesis and medicinal chemistry applications.

Conflicts of interest

There are no conflicts to declare.

Acknowledgements

References

1 Z. Hong-Cai, J. R. Long and O. M. Yaghi, *Chem. Rev.*, 2012, **112**, 673–674.

2 M. E. Davis, *Nature*, 2002, **417**, 813–821.

3 K. Ariga, A. Vinu, Y. Yamauchi, Q. Ji and J. P. Hill, *Bull. Chem. Soc. Jpn.*, 2012, **85**, 1–11.

4 Y. Yamauchi, N. Suzuki, L. Radhakrishnan and L. Wang, *Chem. Rec.*, 2009, **9**, 321–339.

5 M. A. Ghasemzadeh, B. Mirhosseini-Eshkevari, M. Tavakoli and F. Zamani, *Green Chem.*, 2020, **22**, 7265–7300.

6 H. M. A. Hassan, M. A. Betiha, S. K. Mohamed, E. A. El-Sharkawy and E. A. Ahmed, *J. Mol. Liq.*, 2017, **236**, 385–394.

7 M. Samy El-Shall, V. Abdelsayed, A. El R. S. Khder, H. M. A. Hassan, H. M. El-Kaderi and E. T. Reich, *J. Mater. Chem.*, 2009, **19**, 7625–7631.

8 H. M. A. Hassan, M. A. Betiha, S. K. Mohamed, E. A. El-Sharkawy and E. A. Ahmed, *Appl. Surf. Sci.*, 2017, **412**, 394–404.

9 V. I. Isaeva and L. M. Kustov, *Pet. Chem.*, 2010, **50**, 167–180.

10 P. D. Du, H. T. M. Thanh, T. C. To, H. S. Thang, M. X. Tinh, T. N. Tuyen, T. T. Hoa and D. Q. Khieu, *J. Nanomater.*, 2019, **2019**, 1–15.

11 T. B. Faust and D. M. D'Alessandro, *RSC Adv.*, 2014, **4**, 17498–17512.

12 F. Wei, Q. Ren and Z. Liang, *ChemistrySelect*, 2019, **4**, 5755–5762.

13 M. Nasrabadi, M. A. Ghasemzadeh and M. R. Zand Monfared, *New J. Chem.*, 2019, **43**, 16033–16040.

14 W. Chaikittisilp, K. Ariga and Y. Yamauchi, *J. Mater. Chem.*, 2013, **1**, 14–19.

15 N. L. Torad, M. Hu, Sh. Ishihara, H. Sukegawa, A. A. Belik, M. Imura, K. Ariga, Y. Sakka and Y. Yamauchi, *Small*, 2014, **10**, 2096–2107.

16 S. A. Hassan, A. M. Al-Sabagh, N. H. Shalaby, S. A. Hanafi and H. A. Hassan, *Egypt. J. Pet.*, 2013, **22**, 179–188.

17 H. M. Hassan, M. A. Betiha, S. K. Mohamed, E. El-Sharkawy and E. A. Ahmed, *Appl. Surf. Sci.*, 2017, **412**, 394–404.

18 Y. C. Sharma, B. Singh and J. Korstad, *Biofuels, Bioprod. Biorefin.*, 2011, **5**, 69–92.

19 H. C. Zhou, J. R. Long and O. M. Yaghi, *Chem. Rev.*, 2012, **112**, 673–674.

20 H. M. Hassan, M. A. Betiha, S. K. Abd El Rahman, M. Mostafa and M. Gallab, *J. Porous Mater.*, 2016, **23**, 1339–1351.

21 W. R. Mohamed, S. S. Metwally, H. A. Ibrahim, E. A. El-Sherief, H. S. Mekhamer, I. M. Moustafa and E. M. Mabrouk, *J. Mol. Liq.*, 2017, **236**, 9–17.

22 H. M. Savanur, R. G. Kalkhambkar, G. Aridoss and K. K. Laali, *Tetrahedron Lett.*, 2016, **57**, 3029–3035.

23 R. Kore and R. Srivastava, *J. Mol. Catal. A: Chem.*, 2011, **345**, 117–126.

24 R. L. Vekariya, *J. Mol. Liq.*, 2017, **227**, 44–60.

25 A. Dömling and I. Ugi, *Chem. Eng. [Int. Ed.]*, 2000, **39**, 3168–3210.

26 D. A. Ibrahim and A. M. El-Metwally, *Eur. J. Med. Chem.*, 2010, **45**, 1158–1166.

27 M. J. Aliaga, D. J. Ramon and M. Yus, *Org. Biomol. Chem.*, 2010, **8**, 43–46.

28 M. H. Mosslemin and M. R. Nateghi, *Ultrason. Sonochem.*, 2010, **17**, 162–167.

29 G. M. Ziarani, P. Ghlamzadeh, A. Badiei, S. H. Asadi and A. A. Soorki, *J. Chil. Chem. Soc.*, 2015, **60**, 2975–2978.

30 K. T. Patil, P. P. Warekar, P. T. Patil, S. S. Undare, G. B. Kolekar and P. V. Anbhule, *J. Heterocycl. Chem.*, 2018, **55**, 154–160.

31 H. Saeidiroshan and L. Moradi, *J. Organomet. Chem.*, 2019, **893**, 1–10.

32 I. Yavari and M. Esnaashari, *Synthesis*, 2005, **7**, 1049–1051.

33 M. A. Ghasemzadeh, M. H. Abdollahi-Basr and B. Mirhosseini-Eshkevari, *Green Chem. Lett. Rev.*, 2018, **11**, 47–53.

34 M. A. Ghasemzadeh, B. Mirhosseini-Eshkevari and M. H. Abdollahi-Basr, *Appl. Organomet. Chem.*, 2018, **33**, 4679–4687.

35 B. Mirhosseini-Eshkevari, M. A. Ghasemzadeh and J. Safaei-Ghomi, *Res. Chem. Intermed.*, 2015, **41**, 7703–7715.

36 M. A. Ghasemzadeh, M. Azimi-Nasrabad, S. Farhadi and B. Mirhosseini-Eshkevari, *J. Organomet. Chem.*, 2019, **900**, 120935–120942.

37 C. Férey, C. Mellot-Draznieks, F. Serre, J. Millange, S. S. Dutour and I. A Margiolaki, *Science*, 2005, **309**, 2040–2042.

38 X. Liang and J. Yang, *Green Chem.*, 2010, **12**, 201–204.

39 H. Wei, B. Teo, A. Chakraborty and S. Kayal, *Appl. Therm. Eng.*, 2016, **101**, 891–900.

40 T. Hu, Q. Jia, S. He, S. Shan, H. Su, Y. Zhi and L. He, *J. Alloys Compd.*, 2017, **727**, 114–122.

41 C. P. Cabello, G. Berlier, G. Magnacca, P. Rumori and G. T. Palomino, *CrystEngComm*, 2015, **17**, 430–437.

42 X. Huang, Q. Hu, L. Gao, Q. Hao, P. Wang and D. Qin, *RSC Adv.*, 2018, **8**, 27623–27630.